Research Article | Vol. 25, No. 2 | 23 Jan 2017 | OPTICS EXPRESS 785

Optics EXPRESS

Storage and retrieval of electromagnetic waves with orbital angular momentum via plasmon-induced transparency

ZHENGYANG BAI,[1] DATANG XU,[1] AND GUOXIANG HUANG[1,2,*]

[1]*State Key Laboratory of Precision Spectroscopy, School of Physical and Material Sciences, East China Normal University, Shanghai 200062, China*
[2]*NYU-ECNU Joint Institute of Physics at NYU-Shanghai, Shanghai 200062, China*
[*]*gxhuang@phy.ecnu.edu.cn*

Abstract: We propose a scheme to realize the storage and retrieval of high-dimensional electromagnetic waves with orbital angular momentum (OAM) via plasmon-induced transparency (PIT) in a metamaterial, which consists of an array of meta-atoms constructed by a metallic structure loaded with two varactors. We show that due to PIT effect the system allows the existence of shape-preserving dark-mode plasmonic polaritons, which are mixture of electromagnetic-wave modes and dark oscillatory modes of the meta-atoms and may carry various OAMs. We demonstrate that the slowdown, storage and retrieval of multi-mode electromagnetic waves with OAMs can be achieved through the active manipulation of a control field. Our work raises the possibility for realizing PIT-based spatial multi-mode memory of electromagnetic waves and is promising for practical application of information processing with large capacity by using room-temperature metamaterials.

OCIS codes: (190.5530) Pulse propagation and temporal solitons; (020.1670) Coherent optical effects; (160.3918) Metamaterials.

References and links

1. S. Zhang, D. A. Genov, Y. Wang, M. Liu, and X. Zhang, "Plasmon-induced transparency in metamaterials," Phys. Rev. Lett. **101**, 047401 (2008).
2. N. Papasimakis, V. A. Fedotov, N. I. Zheludev, and S. L. Prosvirnin, "Metamaterial analog of electromagnetically induced transparency," Phys. Rev. Lett. **101**, 253903 (2008).
3. P. Tassin, L. Zhang, T. Koschny, E. N. Economou, and C. M. Soukoulis, "Low-loss metamaterials based on classical electromagnetically induced transparency," Phys. Rev. Lett. **102**, 053901 (2009).
4. R. Singh, C. Rockstuhl, F. Lederer, and W. Zhang, "Coupling between a dark and a bright eigenmode in a terahertz metamaterial," Phys. Rev. B **79**, 085111 (2009).
5. J. Gu, R. Singh, X. Liu, X. Zhang, Y. Ma, S. Zhang, S. A. Maier, Z. Tian, A. K. Azad, H.-T. Chen, A. J. Taylor, J. Han, and W. Zhang, "Active control of electromagnetically induced transparency analogue in terahertz metamaterials," Nat. Commun. **3**, 1151 (2012).
6. N. Liu, L. Langguth, T. Weiss, J. Kästel, M. Fleischhauer, T. Pfau, and H. Giessen, "Plasmonic analogue of electromagnetically induced transparency at the Drude damping limit," Nat. Mat. **8**, 758 (2009).
7. K. L. Tsakmakidis, M. S. Wartak, J. J. H. Cook, J. M. Hamm, and O. Hess, "Negative-permeability electromagnetically induced transparency and magnetically active metamaterials," Phys. Rev. B **81**, 195128 (2010).
8. N. Liu, M. Hentschel, T. Weiss, A. P. Alivisators, and H. Giessen, "Three-dimensional plasmon rulers," Science **332**, 1407 (2011).
9. M. Lawrence, N. Xu, X. Zhang, L. Cong, J. Han, W. Zhang, and S. Zhang, "Manifestation of $\mathcal{PT}$ symmetry breaking in polarization space with Terahertz tetasurfaces," Phys. Rev. Lett. **113**, 093901 (2014).
10. S. Raza, and S. I. Bozhevolnyi, "Slow-light plasmonic metamaterial based on dressed-state analog of electromagnetically induced transparency," Opt. Lett. **40**, 4253 (2015).
11. Z. Bai, G. Huang, L. Liu, and S. Zhang, "Giant Kerr nonlinearity and low-power gigahertz solitons via plasmon-induced transparency," Sci. Rep. **5**, 13780 (2015).
12. Z. Bai and G. Huang, "Plasmon dromions in a metamaterial via plasmon-induced transparency," Phys. Rev. A **93**, 013818 (2016).
13. M. Fleischhauer, A. Imamoglu, and J. P. Marangos, "Electromagnetically induced transparency: Optics in coherent media," Rev. Mod. Phys. **77**, 633 (2005).
14. A. I. Lvovsky, B. C. Sanders, and W. Tittel, "Optical quantum memory," Nat. Photon. **3**, 706 (2009).

#281227 http://dx.doi.org/10.1364/OE.25.000785
Journal © 2017 Received 21 Nov 2016; revised 2 Jan 2017; accepted 2 Jan 2017; published 10 Jan 2017

Optics EXPRESS

15. N. Sangouard, C. Simon, H. de Riedmatten, and N. Gisin, "Quantum repeaters based on atomic ensembles and linear optics," Rev. Mod. Phys. **83**, 33 (2011).
16. F. Bussiéres, N. Sangouarda, M. Afzeliusa, H. de Riedmattenb, C. Simon, and W. Tittel, "Prospective applications of optical quantum memories," J. Mod. Opt. **60**, 1519 (2013).
17. M. Fleischhauer and M. D. Lukin, "Dark-state polaritons in electromagnetically induced transparency," Phys. Rev. Lett. **84**, 5094 (2000).
18. Z. Dutton, and J. Ruostekoski, "Transfer and storage of vortex states in light and matterwaves," Phys. Rev. Lett. **93**, 193602 (2004).
19. A. V. Gorshkov, A. André, M. Fleischhauer, A. S. Sørensen and M. D. Lukin, "Universal approach to optimal photon storage in atomic media," Phys. Rev. Lett. **98**, 123601 (2007).
20. O. Firstenberg, M. Shuker, R. Pugatch, D. R. Fredkin, N. Davidson, A. R. Dutton, and J. Ruostekoski, "Theory of thermal motion in electromagnetically induced transparency: effects of diffusion, doppler broadening, and Dicke and Ramsey narrowing," Phys. Rev. A **77**, 043830 (2008).
21. J. Nunn, K. Reim, K. C. Lee, V. O. Lorenz, B. J. Sussman, I. A. Walmsley, and D. Jaksch, "Multimode memories in atomic ensembles," Phys. Rev. Lett. **101**, 260502 (2008).
22. E. Zeuthen, A. Grodecka-Grad, and A. S. Sørensen, "Three-dimensional theory of quantum memories based on Λ-type atomic ensembles," Phys. Rev. A **84**, 043838 (2011).
23. N. Lauk, C. O'Brien, and M. Fleischhauer, "Fidelity of photon propagation in electromagnetically induced transparency in the presence of four-wave mixing," Phys. Rev. A **88**, 013823 (2013).
24. M. Moos, M. Honing, R. Unanyan, and M. Fleischhauer, "Many-body physics of Rydberg dark-state polaritons in the strongly interacting regime," Phys. Rev. A **92**, 053846 (2015).
25. Y. Chen, Z. Bai, and G. Huang, "Ultraslow optical solitons and their storage and retrieval in an ultracold ladder-type atomic system," Phys. Rev. A **89**, 023835 (2014).
26. Y. Chen, Z. Chen, and G. Huang, "Storage and retrieval of vector optical solitons via double electromagnetically induced transparency," Phys. Rev. A **91**, 023820 (2015).
27. C. Liu, Z. Dutton, C. H. Behroozi, and L. V. Hau, "Observation of coherent optical information storage in an atomic medium using halted light pulses," Nature **409**, 490 (2001).
28. R. Pugatch, M. Shuker, O. Firstenberg, A. Ron, and N. Davidson "Topological stability of stored optical vortices," Phys. Rev. Lett. **98**, 203601 (2007).
29. P. K. Vudyasetu, R. M. Camacho, and J. C. Howell, "Storage and retrieval of multimode transverse images in hot atomic rubidium vapor," Phys. Rev. Lett. **100**, 123903 (2008).
30. D. Moretti, D. Felinto, and J. W. R. Tabosa, "Collapses and revivals of stored orbital angular momentum of light in a cold-atom ensemble," Phys. Rev. A **79**, 023825 (2009).
31. U. Schnorrberger, J. D. Thompson, S. Trotzky, R. Pugatch, N. Davidson, S. Kuhr, and I. Bloch, "Electromagnetically induced transparency and light storage in an atomic mott insulator," Phys. Rev. Lett. **103**, 033003 (2009).
32. H.-N. Dai, H. Zhang, S.-J. Yang, T.-M. Zhao, J. Rui, Y.-J. Deng, L. Li, N.-L. Liu, S. Chen, X.-H. Bao, X.-M. Jin, B. Zhao, and J.-W. Pan, "Holographic storage of biphoton entanglement," Phys. Rev. Lett. **108**, 210501 (2012).
33. Y. O. Dudin, L. Li, and A. Kuzmich, "Light storage on the time scale of a minute," Phys. Rev. A **87**, 031801 (2013).
34. J. Wu, Y. Liu, D.-S. Ding, Z.-Y. Zhou, B.-S. Shi, and G.-C. Guo, "Light storage based on four-wave mixing and electromagnetically induced transparency in cold atoms," Phys. Rev. A **87**, 013845 (2013).
35. G. Heinze, C. Hubrich, and T. Halfmann, "Stopped light and image storage by electromagnetically induced transparency up to the regime of one minute," Phys. Rev. Lett. **111**, 033601 (2013).
36. D.-S. Ding, Z.-Y. Zhou, B.-S. Shi and G.-C. Guo, "Single-photon-level quantum image memory based on cold atomic ensembles," Nat. Commun. **4**, 2527 (2013).
37. A. Nicolas, L. Veissier, L. Giner, E. Giacobino, D. Maxein, and J. Laurat, "A quantum memory for orbital angular momentum photonic qubits," Nat. Photon. **8**, 234 (2014).
38. D.-S. Ding, W. Zhang, Z.-Y. Zhou, S. Shi, J.-S. Pan, G.-Y. Xiang, X.-S. Wang, Y.-K. Jiang, B.-S. Shi, and G.-C. Guo, "Toward high-dimensional-state quantum memory in a cold atomic ensemble," Phys. Rev. A **90**, 042301 (2014).
39. D.-S. Ding, W. Zhang, Z.-Y. Zhou, S. Shi, G.-Y. Xiang, X.-S. Wang, Y.-K. Jiang, B.-S. Shi, and G.-C. Guo, "Quantum storage of orbital angular momentum entanglement in an atomic ensemble," Phys. Rev. Lett. **114**, 050502 (2015).
40. L. Allen, M. W. Beijersbergen, R. J. C. Spreeuw, and J. P. Woerdman "Orbital angular momentum of light and the transformation of Laguerre-Gaussian laser modes," Phys. Rev. A **45**, 8185 (1992).
41. D. L. Andrews, and M. Babiker,*The Angular Momentum of Light* (Cambridge University).
42. T. Nakanishi, and M. Kitano, "Implementation of electromagnetically induced transparency in a metamaterial controlled with auxiliary waves," Phys. Rev. Applied **4**, 024013 (2015).
43. T. Nakanishi, T. Otani, Y. Tamayama, and M. Kitano, "Storage of electromagnetic waves in a metamaterial that mimics electromagnetically induced absorption in plasmonics," Phys. Rev. B **87**, 161110 (2013).
44. M. O. Scully and M. S. Zubairy, *Quantum Optics* (Cambridge University).
45. With such notations the frequency and wavenumber of the signal field are given by $\omega_p+\omega$ and k_p+K, respectively. Thus $\omega=0$ corresponds to the center frequency of the signal field.
46. L. Esaki, "New phenomenon in narrow germanium p-n junctions," Phys. Rev. **109**, 603 (1958).
47. T. Jiang, K. Chang, L.-M. Si, L. Ran, and H. Xin, "Active microwave negative-index metamaterial transmission line

Optics EXPRESS

with gain," Phys. Rev. Lett. **107**, 205503 (2011).
48. N. Lazarides and G. P. Tsironis, "Gain-driven discrete breathers in PT-symmetric nonlinear metamaterials," Phys. Rev. Lett. **110**, 053901 (2013).

1. Intruduction

Recently, considerable attention has been paid to the investigation on plasmon-induced transparency (PIT) [1–4], an interesting destructive interference effect arising from the strong coupling between wide-band bright oscillatory mode and narrow-band dark oscillatory mode of the meta-atoms in plasmonic metamaterials. PIT can not only be used to significantly suppress the radiative loss of metamaterials, but also bring steep dispersion and hence large reduction of the propagation velocity of plasmonic polaritons. PIT may occur in a wide range of frequency spectra, from microwave [2], terahertz radiation [3–5], to infrared and visible light [1,6]. Due to its many attractive properties and abundant capabilities for manipulating electromagnetic (EM) radiations, PIT has very promising applications, including the acquisition of lowloss metamaterials [3, 7], optical buffers [5, 8], $\mathcal{PT}$-symmetric metasurfaces [9], slow-light components [10], giant Kerr nonlinear effects [11, 12], and so on.

PIT is a classical analog of the electromagnetically induced transparency (EIT) [13] occurring in gaseous three-level Λ-type or ladder-type atomic systems, where the absorption of a probe laser field due to spontaneous emission can be largely eliminated by the quantum interference effect induced by a control laser field. One of the most important applications of EIT is optical quantum memory, a key technique for quantum information processing [13–16]. Up to now, many theoretical [17–26] and experimental [27–39] researches on light storage and retrieval via EIT have been reported. However, EIT in atomic systems often requires special and often cumbersome experimental conditions, such as large device size and ultracold temperature, which hampers compact chip-integrated applications working at room temperature; additionally, the EIT bandwidth in atomic systems is generally narrow ($\sim$MHz), and hence it is hard to achieve broadband memory based on atomic EIT.

In this work, we propose a scheme to realize the storage and retrieval of EM waves with orbital angular momentums (OAMs) [40, 41] via PIT. The system we consider is a plasmonic metamaterial, which consists of an array of meta-atoms constructed by a metallic structure loaded with two varactors. In a recent experiment, the PIT in such meta-atoms has been demonstrated by Nakanishi and Kitano [42], in which an important technique for actively manipulating the PIT transparency window using a control wave has been proposed. We find that, based on the PIT effect, shape-preserving *dark-mode plasmonic polaritons* carrying various OAMs can be generated, which are mixture of EM-wave modes and dark oscillatory modes of the meta-atoms combined with spatial Laguerre-Gaussian (LG) beams. We show that the multi-mode EM waves with OAMs can have very slow group velocity, and may be stored and retrieved through the switching off and on of a control field. We also suggest a method to increase the memory efficiency of the multi-mode EM waves by using a gain to compensate for the Ohmic loss of the metamaterial.

Before preceding, we note that a study on the storage of EM waves via a PIT has been reported recently by Nakanishi *et al.* [43], where the induced transparency and the storage of EM waves were implemented by applying a bias voltage to the two diodes in the meta-atom through adjusting their capacities. However, such scheme, indicated in [42], cannot completely mimic the EIT in atomic systems because the control field used is a static electric field; furthermore, since the static control field cannot propagate and has to be individually fed to each meta-atom via a bias circuit, it is difficult to increase the number of meta-atoms in the metamaterial [42] and to realize a PIT-based storage. In our work reported below, the control field used is a time-dependent EM wave, which can propagate in space and hence to the all meta-atoms in the metamaterial, and the number of meta-atoms in the metamaterial can be made large enough.

Optics EXPRESS

Thus the PIT and the PIT-based storage here can mimic the EIT and EIT-based storage in atomic systems excellently. In addition, different from Ref. [43] in which only the storage of single-mode EM waves was explored, here we consider the storage of multi-mode EM waves with OAMs.

We also note that EIT-based spatial multi-mode photon memory through LG beams carrying OAMs has been investigated both theoretically and experimentally by using atomic gases as storage media [18, 20, 22, 28–30, 36–39]. However, to the best of our knowledge, up to now no work has been reported on *PIT-based spatial multi-mode EM-wave memory*. Our work described herein provides the possibility for realizing the PIT-based spatial multi-mode EM-wave memory by using a solid metamaterial, which can work at room temperature. Since the bandwidth ($\sim$ GHz) of the transparency window of the PIT proposed here is much wider than that of the EIT in atomic systems (see below), the PIT-based EM-wave memory has advantages not possessing by EIT-based photon memory. Furthermore, because the multi-mode EM waves with OAMs can carry a large amount of information, the storage of such EM waves may lead to a significant improvement for memory capacity, which is desirable for future information processing.

The remainder of the article is organized as follow. Section 2 presents the theoretical model describing the EM waves and the meta-atoms, and derives their coupled equations of motion. Section 3 gives detailed results on the PIT, dark-mode plasmonic polaritons with OAMs, and the storage and retrieval of multi-mode EM waves. The case of nonuniform control field is also discussed. The last section summaries the main results obtained in this work.

2. Model and equations of motion

The metamaterial structure considered here is an array of meta-atoms (unit cells) consisting of a metallic structure loaded with the two varactors on two arms [42]; see Figs. 1(a) and (c). We assume that a pulsed signal field is incident along z direction with the polarization direction along x axis (i.e. collimated on a metamaterial array with the electric field parallel to the arm of unit cells), and a continuous-wave control field is incident along x direction [Fig. 1(c)]. Both the signal and control fields are EM waves with frequency at order of GHz. The varactor on the left (right) arm in the meta-atom has variable capacitance $C_L = C_0 - C_1(t)$ [$C_R = C_0 + C_1(t)$], and can be actively manipulated by the control field [42]. The meta-atom can be well modelled as an RLC circuit with external excitation, as sketched in Fig. 1(b), where the circuit elements R and r_t are radiation resistances, C is the capacitance between neighboring meta-atoms in the vertical direction, and L is the inductance of each metallic arm. The electromotive voltage V is induced by the incident signal field that is parallel to the arm.

The equations of motion for q_L and q_R (i.e. the charges respectively at the varactors on the left and right arms of the meta-atom) can be obtained by adopting the Kirchhoff voltage law, which can be written as

$$L\frac{d^2q_L}{dt^2} + R\frac{d(q_R+q_L)}{dt} + r_t\frac{dq_L}{dt} + \frac{q_R+q_L}{C} + \frac{q_L}{C_L} = V, \tag{1a}$$

$$L\frac{d^2q_R}{dt^2} + R\frac{d(q_R+q_L)}{dt} + r_t\frac{dq_R}{dt} + \frac{q_R+q_L}{C} + \frac{q_R}{C_R} = V, \tag{1b}$$

where the electromotive voltage V is induced by the incident signal field with electric field $E = V/l$, with l the height of the meta-atom unit cell. If assuming the capacitance modulation of the varactors by the control field is small and $C_1(t)$ has the form $C_1(t) = C_M\cos(\omega_c t + \phi)$ ($C_M \ll C_0$), with ω_c the modulation frequency and ϕ a phase constant. Then from Eq. (1) we

Optics EXPRESS

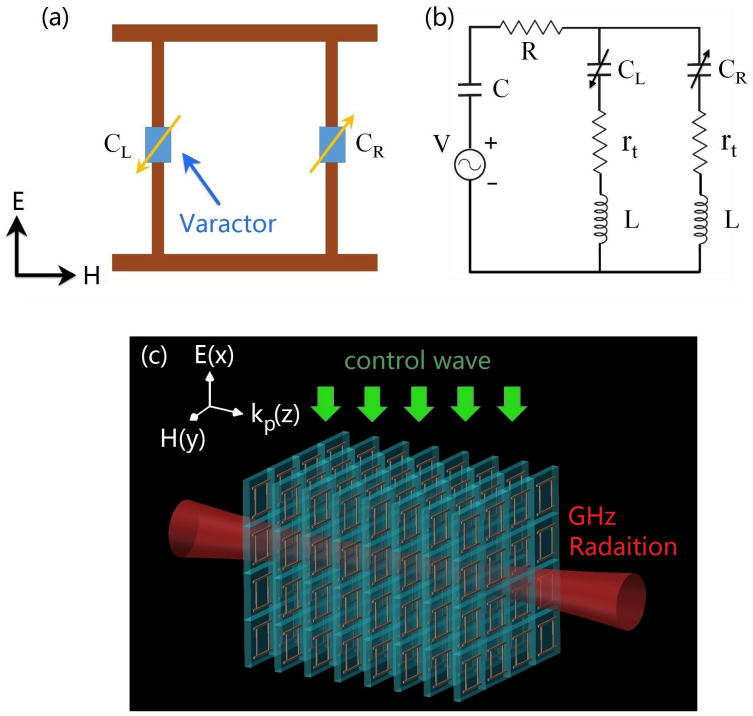

Fig. 1. (a) The meta-atom consisting of a metallic structure loaded with two varactors with capacitance $C_L = C_0 - C_1(t)$ [$C_R = C_0 + C_1(t)$] on its left (right) arm. (b) Equivalent RLC circuit model of the meta-atom. The electromotive voltage V is induced by the incident signal field that is parallel to the arm. R and r_t are radiation resistances, C is the capacitance between neighboring meta-atoms in the vertical direction, and L is the inductance of each metallic arm. (c) Possible experimental arrangement for measuring the propagation of the signal field and multi-mode polarition memory in the PIT metamaterial. The signal (control) field is incident along z (x) direction.

obtain

$$L\frac{d^2q_+}{dt^2} + r\frac{dq_+}{dt} + \frac{q_+}{C'} - \frac{C_M}{C_0^2}\cos(\omega_c t + \phi)q_- = 2El, \tag{2a}$$

$$L\frac{d^2q_-}{dt^2} + r_t\frac{dq_-}{dt} + \frac{q_-}{C_0} - \frac{C_M}{C_0^2}\cos(\omega_c t + \phi)q_+ = 0, \tag{2b}$$

where we have defined $q_\pm = q_R \pm q_L$, $r = 2R + r_t$, and $1/C' = 2/C + 1/C_0$. One sees that, similar to the traditional PIT system [1], q_+ (q_-) acts as a bright (dark) oscillatory mode with the resonant frequency $\omega_r = 1/\sqrt{LC'}$ ($\omega_t = 1/\sqrt{LC_0}$), which couples (does not couple) to the external field E. There is a strong coupling between the bright and dark oscillatory modes under the condition $\omega_c \approx \omega_r - \omega_t$. One can also see that the parameters r and r_t are equivalent radiation resistances of the bright and dark oscillatory modes. In addition, one has $r_t/r << 1$ because the radiation from the bright oscillatory mode is much greater than that from the dark oscillatory mode.

The equation of motion for the electric field E is governed by the Maxwell equation

$$\nabla^2 E - \frac{1}{c^2}\frac{\partial^2 E}{\partial t^2} = \frac{1}{\varepsilon_0 c^2}\frac{\partial^2 P}{\partial t^2}, \tag{3}$$

Optics EXPRESS

with the electric polarization intensity given by $P = \chi_{\rm host}\varepsilon_0 E + N d q_+$, where N is meta-atoms density, d is the effective dipole length for the in-plane oscillation of the bight oscillatory mode, and $\chi_{\rm host}$ is the electric susceptibility of the background material in which the meta-atoms are embedded. Note that when writing the above equation we have assumed that there are N meta-atoms that locate in a unit volume around position $\mathbf{r}$. Since the wavelength of the signal field (~ 300 mm) is much larger than the thickness of the meta-atom unit cell (~ 0.8 mm) [42], the electric field E seen by each meta-atom is nearly homogeneous. Thus it is reasonable to take an electric-dipole approximation, widely used in atomic physics and quantum optics [44], to investigate the dynamics of the system.

We assume the signal field has the form of wavepacket, i.e. $E = \mathcal{E} e^{i(k_p z - \omega_p t)} + \text{c.c.}$, which propagates in the array of the meta-atom layers with the envelope $\mathcal{E}$ [see Fig. 1(c)]. Here $k_p = \omega_p n_D / c$ and $n_D = (1 + \chi_{\rm host})^{1/2}$ is the refractive index of the background material. Taking $q_+ = \tilde{q}_+ e^{i(k_p z - \omega_p t)} + \text{c.c.}$ and $q_- = \tilde{q}_- e^{i[k_p z - (\omega_p - \omega_c)t]} + \text{c.c.}$, here $\tilde{q}_\pm$ represents slowly varying envelops of $q_\pm$, and using slowly varying envelope approximations, from Eq. (2) we obtain

$$\frac{d\tilde{q}_+}{dt} = -(\gamma + i\Delta)\tilde{q}_+ + ig\mathcal{E} + i\Omega_c e^{-i\phi}\tilde{q}'_-, \tag{4a}$$

$$\frac{d\tilde{q}'_-}{dt} = -[\gamma_t + i(\Delta - \delta)]\tilde{q}'_- + i\Omega_c e^{i\phi}\tilde{q}_+, \tag{4b}$$

where $\tilde{q}'_- = \sqrt{\omega_t/\omega_r}\tilde{q}_-$, $g = l/(\omega_r L)$ is the parameter characterizing the coupling strength between the bright oscillatory mode in the meta-atom and the signal field, $\gamma = r/(2L)$ [$\gamma_t = r_t/(2L)$] is the reduced damping rate of the bright (dark) oscillatory mode, $\Delta = \omega_r - \omega_p$ and $\delta = \omega_r - \omega_t - \omega_c$ are quantities representing detunings, $\Omega_c = \omega_t\sqrt{\omega_t/\omega_r}C_M/(4C_0)$ is the "Rabi frequency" of the control field characterizing the coupling strength between the bright oscillatory mode and the dark oscillatory mode, which can be actively changed by adjusting the control field. Expecting no confusion in the reader the primes will be omitted in the following.

The equation of motion for $\mathcal{E}$ can be obtained by the Maxwell Eq. (3), which under slowly varying envelope approximation reduces to

$$i\left(\frac{\partial}{\partial z} + \frac{n_D}{c}\frac{\partial}{\partial t}\right)\mathcal{E} + \frac{1}{2k_p}\nabla_\perp^2\mathcal{E} + \kappa_0\tilde{q}_+ = 0, \tag{5}$$

where $\nabla_\perp^2 = \partial^2/\partial x^2 + \partial^2/\partial y^2$ and $\kappa_0 = (N\omega_p d)/(2\varepsilon_0 n_D c)$. Equations (4) and (5) are similar to the Maxwell-Bloch (MB) equations describing the three-level EIT problem in atomic systems [13, 19].

Since our aim is to investigate the propagation and memory of EM waves with OAMs, we assume the signal field envelope $\mathcal{E}$ can be expanded into the form

$$\mathcal{E}(\mathbf{r}, t) = \sum_{m,p} u_{mp}(r, \varphi, z)\mathcal{E}_{mp}(z, t), \tag{6}$$

where $r = (x^2 + y^2)^{1/2}$ and φ are radial and azimuthal coordinates in a frame of cylindrical coordinate system, $\mathcal{E}_{mp}(z, t)$ are expansion coefficients. The function u_{mp} satisfies the eigen equation $2ik_p\partial u_{mp}/\partial z + \nabla_\perp^2 u_{mp} = 0$, which admits eigen solutions of the form $(\text{LG})_p^m$ modes with orbital angular momentum $m\hbar$ along the z direction, given by Eq. (13). If the diffraction effect of the system plays a negligible role, the $(\text{LG})_p^m$ modes may be approximated by the expression given by (14) (see Appendix A).

It is convenient to express the bright and dark oscillatory modes in the same basis used for

Optics EXPRESS

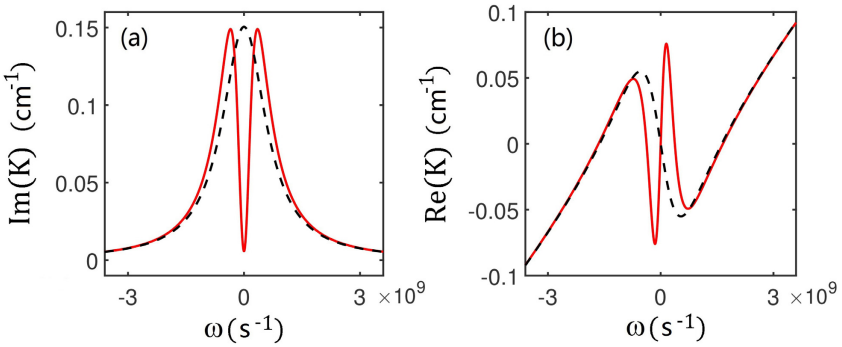

Fig. 2. Linear dispersion relation and PIT in the metamaterial. (a) Im(K), and (b) Re(K) as functions of ω. The dashed and solid lines correspond to the absence ($\Omega_c = 0$) and the presence ($\Omega_c = 0.05\omega_r$) of the control field, respectively.

the signal field, i.e.

$$\tilde{q}_+(\mathbf{r},t) = \sum_{m,p} \tilde{q}_+^{mp}(z,t) u_{mp}(r,\varphi), \tag{7a}$$

$$\tilde{q}_-(\mathbf{r},t) = \sum_{m,p} \tilde{q}_-^{mp}(z,t) u_{mp}(r,\varphi), \tag{7b}$$

where $\tilde{q}_+^{mp}(z,t)$ and $\tilde{q}_-^{mp}(z,t)$ are expansion coefficients. Substituting Eqs. (6) and (7) into the MB Eqs. (4) and (5), multiplying $u_{mp}^*(r,\varphi)$, and making the integration for r and φ, we obtain the MB equations for $\mathcal{E}_{mp}$, $\tilde{q}_+^{mp}$, and $\tilde{q}_-^{mp}$ as follows

$$\frac{d\tilde{q}_+^{mp}}{dt} = -(\gamma + i\Delta)\tilde{q}_+^{mp} + ig\mathcal{E}_{mp} + i\Omega_c e^{-i\phi}\tilde{q}_-^{mp}, \tag{8a}$$

$$\frac{d\tilde{q}_-^{mp}}{dt} = -[\gamma_t + i(\Delta - \delta)]\tilde{q}_-^{mp} + i\Omega_c e^{i\phi}\tilde{q}_+^{mp}, \tag{8b}$$

$$i\left(\frac{\partial}{\partial z} + \frac{n_D}{c}\frac{\partial}{\partial t}\right)\mathcal{E}_{mp}(z,t) + \kappa_0 \tilde{q}_+^{mp}(z,t) = 0. \tag{8c}$$

3. Storage and retrieval of Plasmonic polaritons with OAMs

3.1. PIT characters and dark-mode plasmonic polaritons with OAMs

We now turn to investigate the propagation of the signal field in the system based on the above model. We first consider the case when the control field Rabi frequency $\Omega_c =$ constant. In linear propagation regime, $\mathcal{E}_{mp}$ is a small quantity and takes the form $\mathcal{E}_{mp} = F_{mp}e^{i(Kz-\omega t)}$, where F_{mp} is a yet to be determined envelope function [45]. From Eq. (8), it is easy to get the linear dispersion relation of the system

$$K(\omega) = \frac{n_D}{c}\omega + \frac{\kappa_0 g(\omega - \Delta + \delta + i\gamma_t)}{\Omega_c^2 - (\omega - \Delta + i\gamma)(\omega - \Delta + \delta + i\gamma_t)}, \tag{9}$$

which is similar to that obtained in a Λ-type three-level atomic system [13].

Shown in Fig. 2(a) is the absorption spectrum Im(K) (i.e. the imaginary part of K) of the signal field as a function of ω for $\Delta = \delta = 0$. The dashed and solid lines correspond, respectively, to the absence ($\Omega_c = 0$) and the presence ($\Omega_c = 0.05\omega_r$) of the control field. When plotting the figure, the system parameters used are [42] $\gamma = 0.1\omega_r$, $\gamma_t = 10^{-3}\omega_r$, $\omega_t = 0.7\omega_r$,

Optics EXPRESS

$\omega_c = 0.3\omega_r$, $g = 2.08 \times 10^3$ F$\cdot$ cm/s, $\kappa_0 = 5 \times 10^4\,\mathrm{cm}^{-2}\mathrm{F}^{-1}$, and $\omega_r = 2\pi \times 1.1$ GHz. From the figure we see that, when $\Omega_c = 0$ the signal field has a significant absorption (the dashed line), whereas for $\Omega_c = 0.05\omega_r$ a transparency window is opened (the solid line), which means that the signal field can propagate in the system with negligible absorption. Such phenomenon, similar to the EIT in atomic systems [13], is one of basic characters of PIT. It is easy to show that the PIT condition [i.e. a deep transparency window is opened in Im(K)] of the system is given by $\Omega_c^2 \gg \gamma\gamma_t$.

Figure 2(b) shows the dispersion spectrum Re(K) (i.e. the real part of K) of the signal field as a function of ω, also for $\Delta = \delta = 0$. The dashed and solid lines correspond to $\Omega_c = 0$ and $\Omega_c = 0.05\omega_r$, respectively. We see that when the control field is increased from zero to a finite value, the slope of Re(K) is drastically changed and steepened (the solid line). As a result, the system is changed from an anomalous dispersion regime to a normal one, and hence the group velocity V_g of the signal field is changed from superluminal to subluminal. For the solid line (normal dispersion regime), using the parameters given above we obtain $V_g = 0.039c/n_D$, which is $2.6 \times 10^{-2}\,c$ for $n_D = 1.5$ (for silicon), much slower comparing with the light speed in vacuum.

All the PIT characters illustrated in Fig. 2(a) and Fig. 2(b) are resulted from the strong coupling (and hence the interference effect) between the bright and the dark oscillatory modes in the meta-atoms of the system, induced by the control field Ω_c. It is easy to show that the width of the PIT transparency window is given by the formula $2\Omega_c^2/\gamma$, which is around 0.346 GHz in the present system. Consequently, the PIT transparency window in the present metamaterial is much larger than that obtained in EIT-based atomic systems ($\sim$MHz) [13], which means that the PIT in the metamaterial, at least in the sense of the available bandwidth, is superior to the EIT in atomic systems for the implementation of broadband information processing and transmission.

For obtaining an insight on the signal-field memory before a detailed numerical simulation given below, we consider a case with $\gamma_t = 0$ and the control field being a slow varying function of t. From Eq. (8) we have $\tilde{q}_+^{mp} \approx \frac{ig}{\Omega_c(t)} \frac{\partial}{\partial t} \left(\frac{\mathcal{E}_{mp}(z,t)}{\Omega_c(t)} \right)$ and

$$\left(\frac{\partial}{\partial t} + \frac{c}{n_D} \cos^2\theta(t) \frac{\partial}{\partial z} \right) P_{mp}(z,t) = 0, \tag{10}$$

where $P_{mp}(z,t) = \cos\theta(t)\mathcal{E}_{mp}(z,t) - \sin\theta(t)\sqrt{\frac{\kappa_0 c}{g n_D}}\tilde{q}_-^{mp}$, with $\cos\theta(t) = \Omega_c(t)/[\Omega_c^2(t) + g\kappa_0 c/n_D]^{1/2}$ and $\sin\theta(t) = [g\kappa_0 c/n_D]^{1/2}/[\Omega_c^2(t) + g\kappa_0 c/n_D]^{1/2}$. There are two main features for the function $P_{mp}(z,t)$. First, it is a linear combination between the EM signal field $\mathcal{E}_{mp}(z,t)$ and the dark-mode oscillator $\tilde{q}_-^{mp}$. Second, it is shape-preserved during propagation, with the propagation velocity $V_g(t) = (c/n_D)\cos^2\theta(t)$, which can becomes zero through manipulating $\Omega_c(t)$. We called such combined (hybrid) excitation the *dark-mode plasmonic polariton*, which provides the possibility of EM wave memory in the system. Note that such polariton carries OAMs because the complete combination function including the transverse $(\mathrm{LG})_p^m$ modes is given by $P_{mp}(z,t)\,u_{mp}(r,\varphi)$.

3.2. Storage and retrieval of multi-mode EM waves

Now we consider the storage and retrieval of the multi-mode EM waves in the system. To this end, we make numerical simulation based on the MB equation (8) by manipulating the switching-off and switching-on of the control field. Shown in Fig. 3(a) is the result of the simulation on the storage and retrieval of the signal field $|\mathcal{E}_{mp}|/\mathcal{E}_0$ as a function of z and t/τ_0. In

Optics EXPRESS

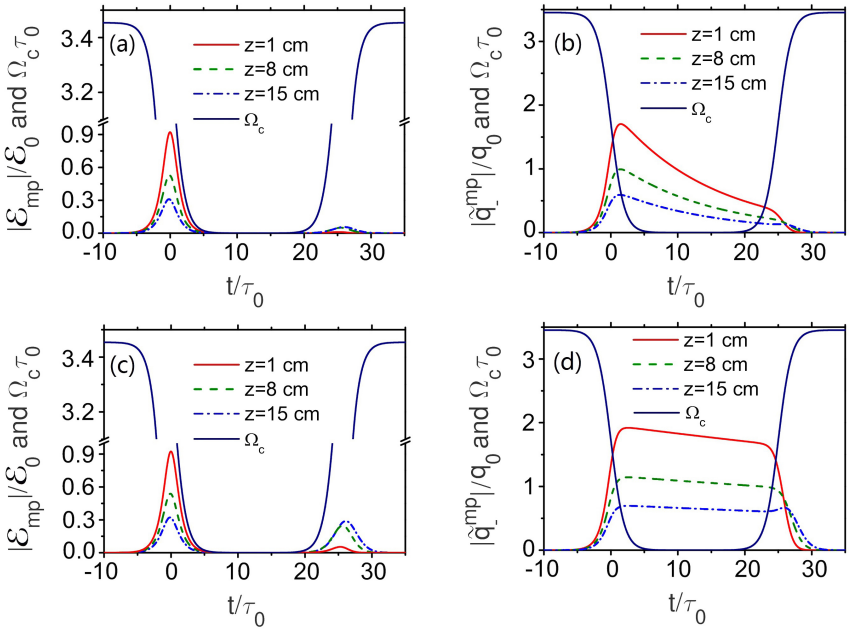

Fig. 3. Storage and retrieval of the signal pulse. Evolutions of the signal field $|\mathcal{E}_{mp}|/\mathcal{E}_0$ (a) and the dark-mode oscillation $|\tilde{q}_-^{mp}|/q_0$ (b) as functions of z and t/τ_0 for $\gamma_t = 10^{-3}\omega_r$. (c) and (d) show, respectively, the evolutions of $|\mathcal{E}_{mp}|/\mathcal{E}_0$ and $|\tilde{q}_-^{mp}|/q_0$ as functions of z and t/τ_0 for $\gamma_t = 10^{-4}\omega_r$. The red solid, green dashed, and blue dashed-dotted lines are for $z = 1$ cm, 8 cm, and 15 cm, respectively. The control field $\Omega_c\tau_0$ is switched off at $t = T_{\rm off} = 0$ and switched on at $t = T_{\rm on} = 25\tau_0$ with $\tau_0 = 10$ ns, shown by blue solid line in each panel.

the simulation, a slowly varying "switching function" for $\Omega_c(t)$ is used, with the form

$$\Omega_c(t) = \Omega_{c0}\left[1 - \frac{1}{2}\tanh\frac{(t-T_{\rm off})}{T_s} + \frac{1}{2}\tanh\frac{(t-T_{\rm on})}{T_s}\right], \tag{11}$$

where $T_{\rm off}$ and $T_{\rm on}$ are respectively times of switching-off and switching-on of the control field. The storage time (or called storage period) of the signal field is approximately given by $t_s = T_{\rm on} - T_{\rm off}$. Here we select $T_s = 2\tau_0$, $T_{\rm off} = 0$, $T_{\rm on} = 25\tau_0$, and $\tau_0 = 10$ ns (pulse width of the signal field), and other system parameters are the same as those used in Fig. 2. The red solid, green dashed, and blue dashed-dotted lines in the figure are for $z = 1$ cm, 8 cm, and 15 cm, respectively. We observe that the storage and retrieval of the signal field can be implemented, with however the retrieved pulse suffering an obvious attenuation comparing with the one before the storage, which is due to the large value of $\gamma_t = 10^{-3}\omega_r = 3.45 \times 10^6\,{\rm s}^{-1}$, inherent in the dark-mode oscillator in the meta-atoms.

Figure 3(b) shows the amplitude of the dark-mode oscillation, $\tilde{q}_-^{mp}$, as a function of z and t/τ_0. The red solid, green dashed, and blue dashed-dotted lines in the figure are respectively for $z = 1$ cm, 8 cm, and 15 cm. We see that $\tilde{q}_-^{mp}$ is nonzero during the storage stage (period) of the signal field, which means that the information in the signal field has been converted into the dark-mode oscillator during the storage stage. Due to the large value of γ_t, $\tilde{q}_-^{mp}$ has also an obvious attenuation as time increases, making the PIT-based storage with a finite lifetime.

Illustrated in Fig. 3(c) and Fig. 3(d) are, respectively, $|\mathcal{E}_{mp}|/\mathcal{E}_0$ and $|\tilde{q}_-^{mp}|/q_0$ as functions of z and t/τ_0 for a smaller damping rate of the dark-mode oscillator, i.e. $\gamma_t = 10^{-4}\omega_r = 3.45 \times 10^5\,{\rm s}^{-1}$. The red solid, green dashed, and blue dashed-dotted lines are for $z = 1$ cm, 8

Optics EXPRESS

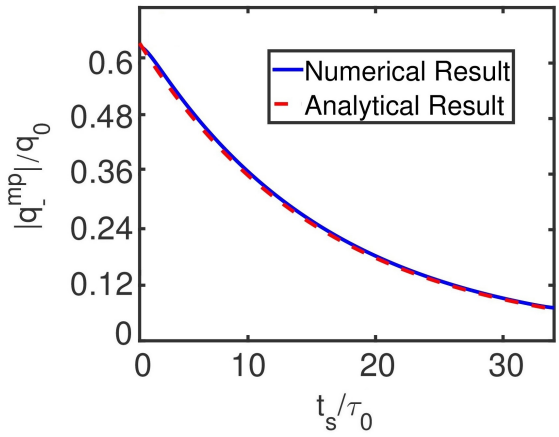

Fig. 4. Dark-mode oscillation $|\tilde{q}_-^{mp}|/q_0$ as a function of (dimensionless) storage time t_s/τ_0 for $z = 15$ cm. The blue solid and red dashed lines are obtained by numerical and analytical results, respectively.

cm, and 15 cm, respectively. We see that in this case the retrieved $|\mathcal{E}_{mp}|/\mathcal{E}_0$ and $|\tilde{q}_-^{mp}|/q_0$ during the storage stage have larger amplitudes, i.e. the lifetime of the storage is longer than that shown in Fig. 3(a) and Fig. 3(b).

In addition to the damping rate γ_t of the dark-mode oscillator, the lifetime of the PIT-based storage depends also on the storage time $t_s = T_{\rm on} - T_{\rm off}$, i.e. on the time difference between the switching-off and switching-on of the control field. Figure 4 shows the result on the dark-mode oscillation $|\tilde{q}_-^{mp}|/q_0$ as a function of (dimensionless) storage time t_s/τ_0 for $z = 15$ cm. The blue solid (red dashed) line is obtained by numerical (analytical) calculation, respectively. One sees that $|\tilde{q}_-^{mp}|/q_0$ decays as the storage time t_s/τ_0 is increased.

From the above results, we know that for a given storage time t_s, which is chosen according to actual demand, the quality of the PIT-based EM-wave memory is determined by the damping rate γ_t of the dark-mode oscillator. The existence of γ_t is mainly due to large Ohmic loss, which however can be suppressed by introducing gain elements into the dark-mode oscillator. For instance, one can inset tunneling (Esaki) diodes [46] into the two metallic arms of the meta-atom shown in Fig. 1. The tunneling diodes have negative resistance [47, 48] and hence may provide gain to the PIT metamaterial. The method by using tunneling diodes to compensate the Ohmic loss in metals has been recognized as a promising technique, particular in microwave regime. In this way, one can make γ_t be very small and even take a negative value.

To describe the quality of the PIT-based memory quantitatively, we define the memory efficiency $\eta = \int_{-\infty}^{+\infty} |\mathcal{E}_{\rm out}(z,\tau)|^2 d\tau / \int_{-\infty}^{+\infty} |\mathcal{E}_{\rm in}(\tau)|^2 d\tau$ for a given storage time. Figure 5 shows η as a function of z for the storage time $t_s = T_{\rm on} - T_{\rm off} = 25\tau_0$. The red solid, blue dashed, green dotted and purple dashed-dotted curves in the figure are for γ_t taking $-4.2\times10^{-4}\omega_r$, $-1\times10^{-4}\omega_r$, 0, and $1\times10^{-4}\omega_r$, respectively. From the figure we can obtain the following conclusions: (i) For all γ_t, as z increases the memory efficiency η firstly has a fast growth, then arrives to a peak value, and finally decreases slowly. (ii) The smaller the damping rate γ_t, the larger the peak value of η. For instance, η can reach to 94% at $z = 26.4$ cm for $\gamma_t = -4.2\times10^{-4}\omega_r$. Consequently, one can acquire a high efficiency for the PIT-based memory by embedding gain elements into the metamaterial and using suitable length of the medium.

The storage and retrieval of the three-dimensional signal field are also calculated numerically. Shown in Fig. 6 is the result of the intensity distributions of the signal field with the transversal LG modes in the x-y plane before and after the storage. Panel (a) gives the intensity patterns for

Optics EXPRESS

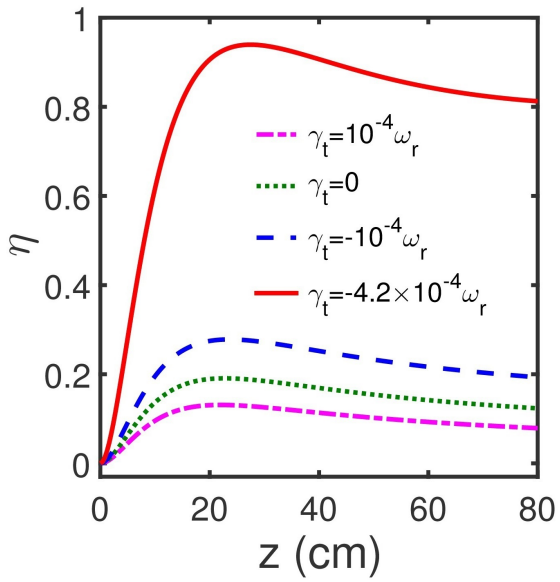

Fig. 5. The PIT-based memory efficiency η as functions of propagation distance z and γ_t for storage time $t_s = 25\tau_0$. Red solid, blue dashed, green dotted and purple dashed-dotted curves are for γ_t taking $-4.2 \times 10^{-4}\omega_r$, $-1 \times 10^{-4}\omega_r$, 0, and $1 \times 10^{-4}\omega_r$, respectively.

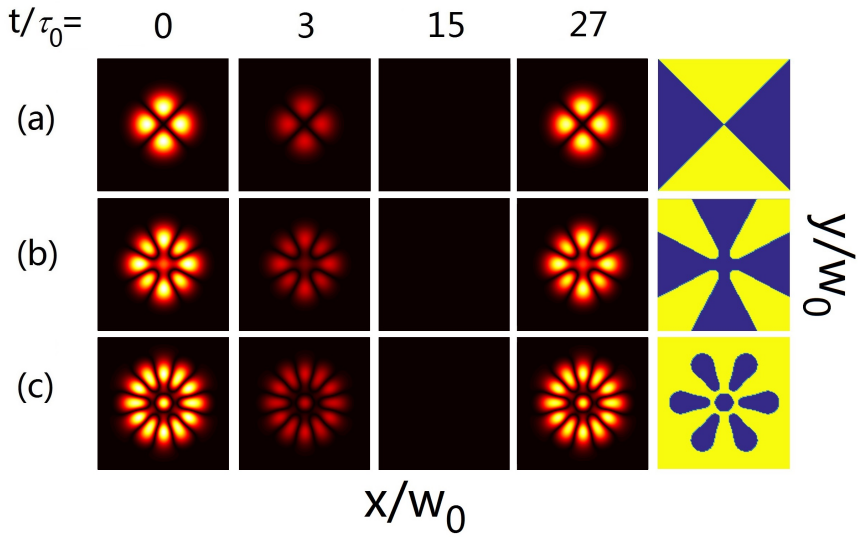

Fig. 6. The storage and retrieval of the three-diemnsional signal field. (a) The intensity patterns for the superposed LG modes $[(\mathrm{LG})_0^2 + (\mathrm{LG})_0^{-2}]$ in the x-y plane respectively at the time $t = 0$, $3\tau_0$, $15\tau_0$, and $27\tau_0$. (b) The same as (a) but for the superposed LG modes $[(\mathrm{LG})_0^4 + (\mathrm{LG})_0^{-4} + (\mathrm{LG})_0^0 + (\mathrm{LG})_2^0]$. (c) The same as (a) but for the superposed LG modes $[(\mathrm{LG})_0^6 + (\mathrm{LG})_0^{-6} + \sum_{p=0}^{5}(\mathrm{LG})_p^0]$. The first column is the patterns before the storage, the second and third columns are the patterns during the storage, and the fourth column is the patterns after the storage. The fifth column shows the phase distribution of the input LG modes.

Optics EXPRESS

the superposition of a set of LG modes $[(\mathrm{LG})_0^2 + (\mathrm{LG})_0^{-2}]$ at the time $t = 0$, $3\tau_0$, $15\tau_0$, and $27\tau_0$, respectively. Panels (b) and (c) give similar intensity patterns as in panel (a), but respectively for the superposed LG modes $[(\mathrm{LG})_0^4 + (\mathrm{LG})_0^{-4} + (\mathrm{LG})_0^0 + (\mathrm{LG})_2^0]$ and $[(\mathrm{LG})_0^6 + (\mathrm{LG})_0^{-6} + \sum_{p=0}^{5}(\mathrm{LG})_p^0]$. In the figure, the first column (for $t = 0$) is the patterns before the storage, the second and third columns (for $t = 3\tau_0$ and $15\tau_0$) are the patterns during the storage, and the fourth column (for $t = 27\tau_0$)is the patterns after the storage. The fifth column shows the phase distribution of the input LG modes.

The above result shows that the multi-mode EM waves with OAMs can be indeed stored and retrieved by actively manipulating the control field. In particular, the phase distribution of the LG modes, which carry OAM information, can also be stored and recovered again. We stress that there is an advantage for the storage of EM waves with OAMs, because the phase distribution of the LG modes, which carry OAM information, can also be stored and recovered during the memory process. Although the Ohmic loss in the dark-mode lowers the amplitude of EM waves, the phase distribution is unaffected during the storage and retrieval.

3.3. Storage and retrieval of the multi-mode EM waves with nonuniform control field

In the above study, the Rabi frequency of the control field, Ω_c, is assumed to be spatially uniform, which makes the EM modes with different OAMs in the meta-material independent in the processes of propagation, storage and retrieval. However, if Ω_c is not spatially uniform, which may be a practical case in experiments, these EM modes will not be independent. In this situation, a coupling between different EM modes occurs and the dynamics in the transverse directions come into play.

To address this question, we replace the time-dependent Rabi frequency $\Omega_c(t)$ of the control field assumed above by a space-time-dependent one with the form $\Omega_c(\mathbf{r}, t) = \Omega_c(t)A(\mathbf{r})$, here $\Omega_c(t)$ is time-dependent amplitude and $A(\mathbf{r})$ is spatial distribution function. Generally, the spatial distribution function is radially symmetric and thus $A(\mathbf{r}) = A(r)$. In this situation, Eq.(8a) and Eq.(8b) are replaced by

$$\frac{d\tilde{q}_+^{mp}}{dt} = -(\gamma + i\Delta)\tilde{q}_+^{mp} + ig\mathcal{E}_{mp} + i\Omega_c(t)e^{-i\phi}\sum_{m'p'} A_{mp,m'p'}\tilde{q}_-^{m'p'}, \tag{12a}$$

$$\frac{d\tilde{q}_-^{mp}}{dt} = -[\gamma_t + i(\Delta - \delta)]\tilde{q}_-^{mp} + i\Omega_c(t)e^{i\phi}\sum_{m'p'} A_{mp,m'p'}\tilde{q}_+^{m'p'}, \tag{12b}$$

where $A_{mp,m'p'} = \int dr d\varphi u_{mp}^*(r,\varphi)A(r)u_{m'p'}(r,\varphi)$ are coupling coefficients.

The PIT property and related EM modes memory of the system can also be calculated using the method the same as that used in the last subsections. For simplicity, we take $A(r) = \exp[-r^2/(nw_0)^2]$, with n the beam-waist ratio between the control field (nw_0) and the signal field (w_0). Shown in Fig. 7 is the result of numerical simulation on the memory efficiency η of the signal field for different transverse (azimuthal) mode index m and the beam-waist ratio n, when the signal field propagates to the distance $z = 12$ cm [panel (a)] and $z = 24$ cm [panel (b)]. The simulation is made based directly on Eqs. (8c), (12a) and (12b). When plotting the figure, we select $\gamma_t = -4.2 \times 10^{-4}\omega_r$, $\Omega_c(t) = 0.05\omega_r\{1 - 0.5\tanh[(t - T_{\mathrm{off}})/T_s] + 0.5\tanh[(t - T_{\mathrm{on}})/T_s]\}$, with other system parameters the same as those used in Fig. 5. From the figure, we see that the PIT-based multi-mode EM wave memory efficiency η in presence of the spatially nonuniform control filed has a dependence on z, m and n, i.e. $\eta = \eta_{mn}(z)$. For given z and n, the memory efficiency $\eta_{mn}(z)$ is larger for smaller m. However, values of $\eta_{mn}(z)$ for different m rapidly approach to an identical value when n is increased. Especially, at $z = 12$ cm ($z = 24$ cm) the memory efficiency reaches to its limit value 71% (93%) only for $n = 6$ ($n = 7$). The limit values in both panels are shown by black dashed lines, obtained by $n \to \infty$. In this limit, $A(r) = 1$ and hence the coupling coefficients reduce to the simple form $A_{mp,m'p'} = \delta_{pp'}\delta_{mm'}$

Optics EXPRESS

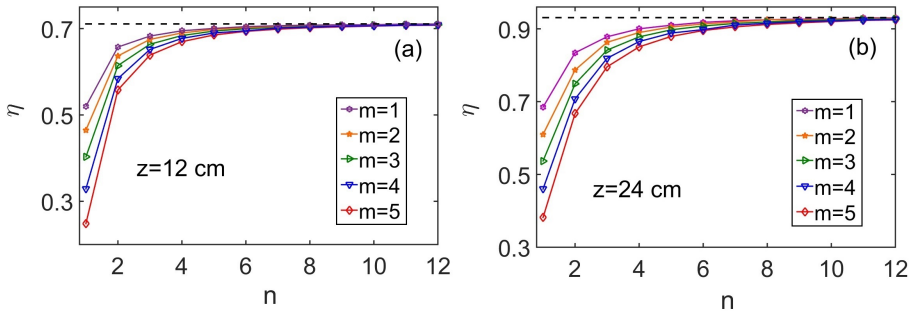

Fig. 7. PIT-based memory efficiency η as a function of the beam-waist ratio n between the control and the signal fields for different transverse (azimuthal) mode index m. Panel (a) [(b)] is for the signal field propagating to the distance $z = 12$ cm ($z = 24$ cm). The dashed black lines denote the case for $n \to \infty$.

due to the orthogonality of the LG modes, and hence the result obtained here returns back to that given in the last subsection. Consequently, we can still realize multi-mode EM wave memory with high fidelity even in the presence of the non-uniform control field. The discussion herein can be also generalized to the case of an inhomogeneous meta-atom density, i.e. $N = N(\mathbf{r})$. Similar conclusion like that shown in Fig. 7 can also be obtained.

4. Discussion and summary

To experimentally realize the propagation, storage and retrieval of the plasmonic polaritons with OAMs via the PIT predicted above, one can employ the system developed in Ref. [42]. In such system, the meta-atoms are manufactured by a structure made of copper, which is fabricated on a print circuit board. The varactor diodes (Infineon BBY52-02W) are inserted at the two arms in each meta-atom (unit cell). Furthermore, one can place the meta-atoms in open-type waveguides, which can effectively interact with the electromagnetic field confined in the waveguides [42], and hence implementing the memory process of the plasmonic polaritons with OAMs in the system.

In summary, in this work we have proposed a scheme for the realization of the storage and retrieval of multi-mode EM waves with OAMs via PIT in a metamaterial consisting of an array of meta-atoms constructed by a metallic structure loaded with two varactors. We have shown that due to the PIT effect the system allows the existence of shape-preserving dark-mode plasmonic polaritons, which are mixture of EM-wave modes and dark oscillatory modes of the meta-atoms and may carry OAMs. We have demonstrated that the slowdown, storage and retrieval of the multi-mode EM waves with OAMs can be obtained through the active manipulation of a control field. The results reported here raise the possibility for realizing high-dimensional spatial multi-mode memory of EM waves via PIT, and are promising for future practical application of information processing with large capacity by using room-temperature metamaterials. It is expected that the PIT-based high-dimensional spatial multi-mode EM-wave memory demonstrated herein can be generalized to terahertz and even optical frequency regimes.

Optics EXPRESS

Appendix

A. Laguerre-Gaussian modes

The function u_{mp} in Eq. (6) satisfies the equation $2ik_p\partial u_{mp}/\partial z + \nabla_\perp^2 u_{mp} = 0$, which admits the eigen solutions [40, 41]

$$u_{mp} = \frac{C_{mp}}{\sqrt{w(z)}}\left(\frac{\sqrt{2}r}{w(z)}\right)^{|m|}\exp\left[-\frac{r^2}{w^2(z)}\right]L_p^{|m|}\left(\frac{2r^2}{w^2(z)}\right)\exp(im\varphi)\exp[i\Phi(z)], \quad (13)$$

where $\Phi(z) = \exp\{-i[\phi_1(z) + \phi_2(z)]\}$ with $\phi_1(z) = k_p r^2 z/[2(z_R^2 + z^2)]$ and $\phi_2(z) = (2p + |m| + 1)\tan^{-1}(z/z_R)$, $L_p^{|m|}$ are the generalized LG polynomials (with m and p respectively azimuthal and radial indices), $w(z) = w_0(1 + z^2/z_R^2)^{1/2}$ is beam radius in the radial direction, and $z_R = w_0^2 k_p/2$ is Rayleigh length.

The eigen solutions (13) with the normalization constant $C_{mp} = \sqrt{2^{|m|+1}p!/[\pi(p + |m|)!]}$, called $(\mathrm{LG})_p^m$ modes, constitute a complete and orthogonal function set, describing a paraxial propagation of the signal field. If we assume the diffraction effect of the system is small (i.e. z_R is large enough) so that $w(z) \approx w_0$, $\Phi(z) \approx 0$, and hence the $(\mathrm{LG})_p^m$ modes can be approximated by [24]

$$u_{mp} = \frac{C_{mp}}{\sqrt{w_0}}\left(\frac{\sqrt{2}r}{w_0}\right)^{|m|}\exp\left(-\frac{r^2}{w_0^2}\right)L_p^{|m|}\left(\frac{2r^2}{w_0^2}\right)\exp(im\varphi). \quad (14)$$

Profiles of the $(\mathrm{LG})_p^m$ modes show concentric rings, the number of which is determined by the mode index p. The mode index m is contained in the azimuthal phase term $\exp(im\varphi)$, which gives rise to $|m|$ intertwined helical wave-fronts, i.e. the surfaces of equal phase. The handedness of these helixes is determined by the sign of m. Since $\hat{L}_z\,(\mathrm{LG})_p^m = m\hbar\,(\mathrm{LG})_p^m$, here $\hat{L}_z = -i\hbar\partial/\partial\varphi$, $(\mathrm{LG})_p^m$ modes carry the OAM with the value $m\hbar$ along z direction, which are usable for information processing with large capacity [40, 41].

Funding

This work was supported by the NSF-China under Grant No. 11474099 and the Chinese Education Ministry Reward for Excellent Doctors in Academics under Grant No. PY2014009.